Energetics of MnO_2 polymorphs in density functional theory

Daniil A. Kitchaev,[1] Haowei Peng,[2] Yun Liu,[1] Jianwei Sun,[2] John P. Perdew,[2,3] and Gerbrand Ceder[1,4,5,*]

[1]*Department of Materials Science and Engineering, Massachusetts Institute of Technology, Cambridge, Massachusetts 02139, USA*

[2]*Department of Physics, Temple University, Philadelphia, Pennsylvania 19122, USA*

[3]*Department of Chemistry, Temple University, Philadelphia, Pennsylvania 19122, USA*

[4]*Department of Materials Science and Engineering, University of California Berkeley, Berkeley, California 94720, USA*

[5]*Materials Science Division, Lawrence Berkeley National Laboratory, Berkeley, California 94720, USA*

(Received 28 November 2015; published 26 January 2016)

We report the energetics and properties of the β, α, R, γ, λ, and δ polymorphs of MnO_2 within density functional theory, comparing the performance of the recently introduced SCAN functional with that of conventional exchange-correlation functionals and experiment. We find that SCAN uniquely yields accurate formation energies and properties across all MnO_2 polymorphs. We explain the superior performance of SCAN based on its satisfaction of all known constraints appropriate to a semilocal exchange-correlation functional and its accurate representation of all types of orbital overlap.

DOI: 10.1103/PhysRevB.93.045132

First-principles thermodynamics has over the last decades matured into a reliable method for accessing the energetics of phase transitions and reactions in condensed matter systems. At the heart of this method lies Kohn-Sham density functional theory (DFT) [1], with its standard approximations to the exchange-correlation energy providing a reasonably accurate picture of electronic structure. One of the most basic results that can be derived from a set of DFT calculations is the ground-state structure of a given compound under some set of conditions, usually set as zero temperature and pressure. However, despite the importance of accurate first-principles structure determination for both materials and property analysis [2–5] this determination is often extremely difficult as the total energy differences between competing phases can be on the order of only a few meV per formula unit [6]. As a result, ground state structure selection is an attractive benchmark for verifying the adequacy of the physical model underlying a given approximation to the exchange-correlation energy.

One particularly interesting system for investigating structure-transition energetics within DFT is the set of manganese oxides. The Mn-O system contains a diverse set of relatively well characterized structures both across a range of stoichiometries (MnO, Mn_3O_4, Mn_2O_3, and MnO_2), and within a single stoichiometry (pyrolusite β, ramsdellite R, hollandite α, intergrowth γ, spinel λ, layered δ MnO_2), as shown in Fig. 1. All the MnO_2 polymorphs share a common basic atomic structure—small Mn^{4+} ions in a spin-polarized $3d^3$ configuration and large, highly polarizable O^{2-} ions in a spin-unpolarized $2p^6$ configuration, arranged in corner- and edge-sharing MnO_6 octahedra. The different packings of these octahedra form a variety of polymorphic structures, many of which have been studied extensively for applications in energy storage, catalysis, pigmentation, etc. [7–15].

The relative stability of the various oxidation states of Mn-O has been previously investigated within the Perdew-Burke-Erzenhof (PBE) and PBE+U forms of GGA-DFT, as well as with the exact-exchange-corrected hybrid PBE0 and Heyd-Scuseria-Erzenhof (HSE) functionals [16]. However, the energetics and properties of the polymorphic phases of MnO_2 remain unresolved in first-principles calculations [17–19]. Experimentally, it is established that pyrolusite β-MnO_2 is the ground state of pure MnO_2 [9], but to our knowledge no nonempirical DFT method has stabilized β-MnO_2 as the ground state of the system. In this report we resolve this problem with the use of the recently reported SCAN meta-GGA [20] and show that the resolution of the ground state structure problem in the MnO_2 system also leads to a much more accurate representation of the basic physics of the material.

A common feature of exchange-correlation functionals is the selective improvement of a target property at the expense of errors elsewhere. To study the accuracy of common DFT methods for structure selection and other key properties in comparison to SCAN [20], we consider the GGAs PBE [21] and PBEsol [22], the Hubbard-U-corrected PBE+U and PBEsol+U [23,24], and the hybrid of PBE with exact exchange HSE06 [25,26] functionals. This set of functionals provides a representative sample of common approaches to improving the accuracy of DFT. PBE is the base workhorse nonempirical functional most commonly used in the literature [27]. While PBE provides reasonably accurate results for total energies across a wide range of chemistries, it suffers from significant electronic structure errors arising from self-interaction, as well as a tendency to disfavor density overlap between atoms (making lattice constants too long, especially in van der Waals bonded systems), originating from a compromise in the representation of the exchange energy of solids and molecules [21,28,29]. A common solution to the self-interaction problem is the empirically fitted Hubbard U correction in PBE+U and PBEsol+U [24,29]. The downsides of the +U approach are that it usually requires fitting to experimental data, and that it gives rise to errors in orbital hybridization, leading to further reduction of density overlap between atoms and errors in

*Corresponding author: gceder@berkeley.edu

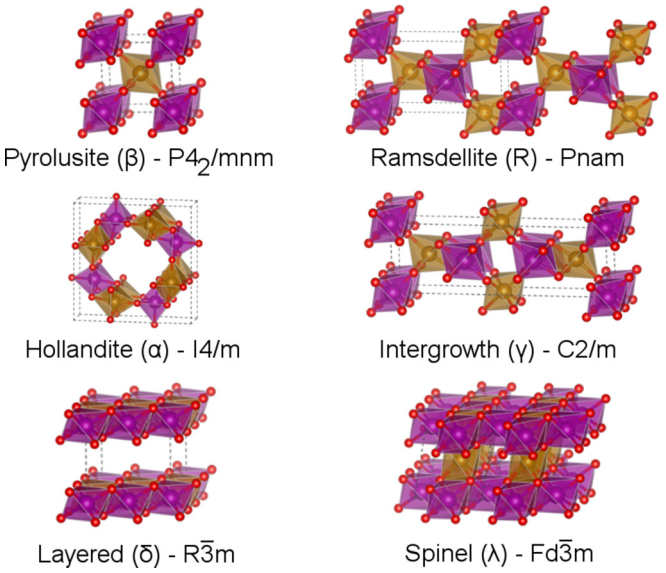

FIG. 1. The polymorphs of MnO_2 with well-defined crystalline phases. The purple and yellow atoms represent spin-up and spin-down Mn, respectively, while the red atoms represent O. The magnetic orderings shown correspond to the lowest-energy configurations within PBE, PBEsol, and SCAN. Note that the space group corresponds to structural symmetry, neglecting reductions of symmetry from the magnetic ordering.

magnetism [30]. The density overlap problem in PBE can be resolved by restoring the second-order gradient coefficient for exchange, as is done in the PBEsol functional [22]. PBEsol improves the general energetic representation of solids and surfaces, but typically *underestimates* lattice parameters and overly stabilizes molecules [31] and solids with respect to atomization. Finally, hybrid functionals such as HSE06 attempt to improve the performance of PBE by introducing a fraction of exact exchange into the calculation [25,26], which cancels some of the self-interaction error, at the cost of a significant increase in computational expense. In contrast, SCAN [20], and other meta-GGAs [32–36], attempt to correct the errors of PBE by introducing the orbital kinetic energy density into the functional, which allows for the simultaneous representation of extended systems and molecules, and enables SCAN to appropriately treat different chemical bonds (e.g., covalent, metallic, and even weak bonds), which no LDA or GGA can [37]. Since the design of SCAN is targeted to satisfy all fundamental constraints simultaneously, rather than correcting specific drawbacks of PBE, we expect that SCAN would yield an overall improvement in the representation of all system properties relative to PBE, rather than the trade-offs in accuracy typical of other functionals.

All calculations were done within the Vienna *ab initio* simulation package [38], using a Γ-centered k-point grid with a reciprocal space discretization of 0.25 $Å^{-1}$. For both PBE+U and PBEsol+U we rely on the Dudarev effective-U formulation [24], applying a $U = 3.9$ eV to the $3d$ states of each Mn atom, based on previous optimizations for the formation energy, redox potential, and agreement with higher-order functionals [16,39]. To obtain the total energy of each phase we chose the supercells given in Table I, in all cases initializing the calculation based on experimentally reported geometries and relaxing the structures self-consistently within each functional. As all MnO_2 phases are known to be well-represented energetically by antiferromagnetic (AFM) orderings [16,19,40–45], we ensured that the chosen supercells were compatible with all likely AFM orderings. To obtain the magnetic structure of each phase, we enumerated up to 12 of the most likely configurations, chosen as the orderings with a net zero magnetic moment and highest symmetry. The magnetic structures used for HSE calculations and all analysis across all functionals are given in Fig. 1 and are the ground state magnetic orderings for PBE, PBEsol, and SCAN, but not PBE+U or PBEsol+U, which we will address below. Subsequent band structure and DOS calculations were set up using the scheme proposed by Setyawan and Curtarolo [46,47], based on the self-consistently relaxed, symmetry-reduced primitive cells derived from the AFM orderings described above.

TABLE I. Experimental parameters for the polymorphs of MnO_2, given for the supercells used for total energy calculations. Uncertainty, given in parentheses, is determined as the standard deviation between experimental results (β, R, α), or assumed uncertainty from diffraction refinement (γ, λ, δ). The formation enthalpy is given with respect to β-MnO_2. References: β [9,12,49–55], R [9,12,52,56–58], α [9,12,52,59], γ [10], λ [11], δ [48,60,61].

Phase	Lattice parameters (a,b,c)(Å)	Volume (Å^3/f.u.)	ΔH_f (meV/f.u.)	E_{gap} (eV)
β	4.39(1), 4.39(1), 2.871(4)	27.8(1)	0	0.27
R	9.29(3), 4.49(4), 2.857(8)	29.8(5)	56(32)	
α	9.80(2), 9.80(2), 2.85(1)	34.2(2)	>0	
γ	13.7(1), 2.86(1), 4.46(1)	29.2(3)	>0	
λ	5.67(1), 5.67(1), 5.67(1)	32.3(1)	>0	
δ	5.69(1), 5.69(1), 7(3)[a]		>0	2.1[b]

[a]The c lattice constant (interlayer spacing) in δ-MnO_2 is highly uncertain as all reported samples of this phase have some amount of intercalated cations or water.

[b]The band gap for δ-MnO_2 measured by Pinaud *et al.* is for birnessite-type δ-MnO_2, but explicitly noting the absence of midgap Mn^{3+} states [48], suggesting it should be similar to that of pure δ-MnO_2.

The formation energies of the various MnO_2 phases with respect to the experimental ground state β-MnO_2 are given in Fig. 2. While the experimental formation enthalpies of most phases are not known, they must be positive in order for β to be the ground state phase. It is clear that only PBEsol and SCAN even qualitatively reproduce this result, and only SCAN is able to quantitatively reproduce the experimentally known formation enthalpy of R-MnO_2. The fact that only PBEsol and SCAN give qualitative agreement with experiment in terms of picking the correct ground state phase could be expected from the fact that SCAN and PBEsol are the only functionals that yield reasonably accurate descriptions of noncovalent electronic density overlaps, which are critically important for distinguishing between the various packings of MnO_6 octahedra that form the diverse polymorphs of MnO_2. However, due to its ability to recognize not only weak electron density overlap but also strong chemical bonds [62], SCAN

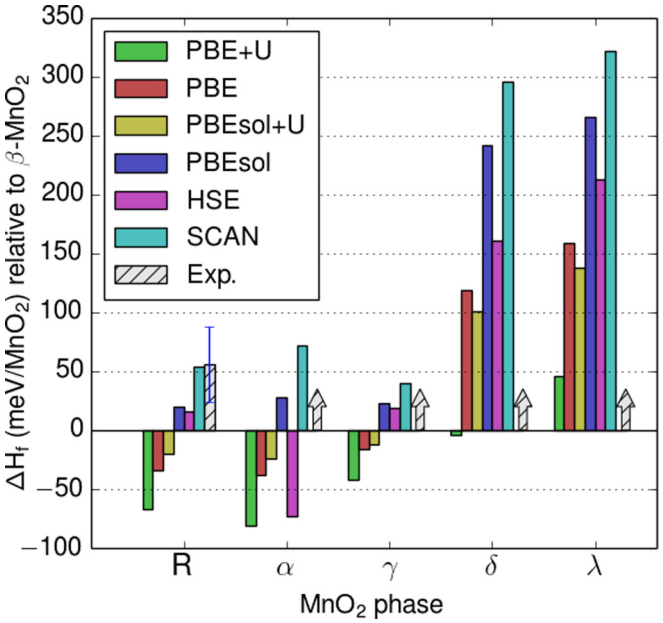

FIG. 2. Formation energies of MnO_2 polymorphs with respect to the experimental ground state β-MnO_2. Only PBEsol and SCAN stabilize β-MnO_2 as the ground state phase, and only SCAN quantitatively agrees with the experimental transition enthalpy from β-MnO_2 to R-MnO_2. Note that the experimental "arrows" drawn for the α, γ, δ, and λ phases indicate that experimentally the formation energy of these phases is some unknown positive quantity.

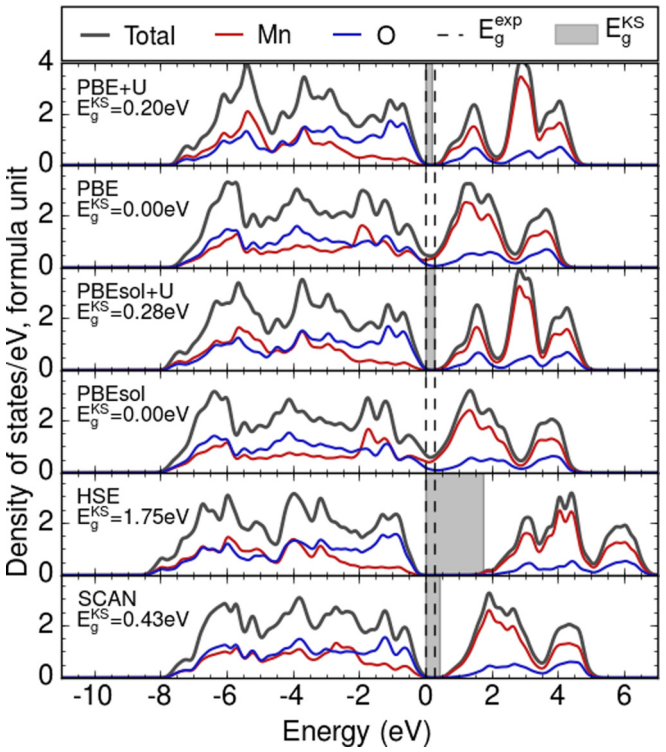

FIG. 3. The total and atom-projected density of states of β-MnO_2. The shaded regions denote the band gap predicted by each functional, while the dotted line marks the experimental band gap, 0.27 eV [54,55]. The DFT band gap is given by the generalized Kohn-Sham eigenvalues from a band structure calculation, while the DOS is calculated with a 0.1 eV smearing.

significantly improves on the successes of PBEsol, giving an altogether more accurate picture of the physics of the MnO_2 system, leading to the remarkable quantitative agreement between experiment and SCAN ($\Delta H_f^{\beta\to R} = 54.2$ meV/MnO_2 from SCAN versus 56 ± 32 meV/MnO_2 experimentally [9]).

In terms of electronic structure, all phases of MnO_2 are semiconducting. However, as can be seen in Fig. 3, both PBE and PBEsol predict β-MnO_2 to be a metal due to the self-interaction error present in both functionals [63], and the resulting reduction of the calculated band gap. The empirical Hubbard U correction opens up a small band gap close to the experimental value (PBE+U: 0.20 eV, PBEsol+U: 0.28 eV, Expt.: 0.27 eV [54,55]), which could be expected as, by construction, the Hubbard U leads to the localization of carriers, flattening of d bands, and opening of band gaps [24]. HSE in turn converges to a much larger band gap (1.7 eV), while SCAN gives a gap (0.43 eV) that is close to the $+U$ and experimental results. The results are similar for the δ phase where the experimental band gap is also known: PBE and PBEsol underestimate the bandgap (1.1 and 0.96 eV, respectively, versus 2.1 eV experimental [48]) PBE+U, PBEsol+U, and SCAN give almost identical band gaps in good agreement with experiment (2.0, 2.1, and 2.0 eV, respectively), and HSE overestimates the band gap (3.4 eV). It must be noted that the experimental band gaps in the MnO_2 system are not definitively established—the gaps reported here are based on the best estimates available in the literature. The fact remains however that SCAN significantly increases the band gap compared to PBE and PBEsol, which are known to underestimate band gaps, and agrees with values obtained from empirically fitted PBE+U and PBEsol+U functionals, while keeping the gaps well below those of HSE. The improvement in band gap could originate from two sources. First, the SCAN meta-GGA, like the hybrid functionals, is implemented in a generalized Kohn-Sham scheme in which the exchange-correlation potential is not a multiplicative operator [62]. Second, the self-interaction error in SCAN is greatly reduced in the case of well-localized electrons as SCAN uses a functional form that is almost self-interaction free in the case of atomiclike densities, where the exchange-correlation hole remains near its reference electron [20]. As the valence band in β-MnO_2 consists of weakly hybridized Mn t_{2g} and O p_z states, this condition may be approximately satisfied, leading to a cancellation of self-interaction in SCAN, and consequently an increased band gap compared to PBE or PBEsol. We must note however that this result is somewhat atypical—we find that for many materials, including rutile TiO_2, SCAN corrects about half of the PBE underestimation of the experimental gap.

Another important property of the MnO_2 system is its magnetic configuration. Experimentally, β-MnO_2 adopts a helical magnetic configuration [64–66] while all other phases are believed to be antiferromagnetic (AFM) [42–45]. In previous DFT work, the ferromagnetic (FM) form of β and α MnO_2 was found to be stable in PBE+U, in conflict with experiment [16,40,41]. We find that both PBE+U and PBEsol+U stabilize FM orderings with respect to the reference AFM

TABLE II. The lattice parameter mean (absolute) relative error (MRE, MARE) of the β, R, α, γ, and λ phases of MnO_2, as compared to the experimental values presented in Table I. It is clear that SCAN performs better than the similarly efficient nonempirical PBE and PBEsol functionals, and is outperformed by only HSE and the empirically fitted PBEsol+U. Note that the δ phase is excluded due to highly uncertain experimental lattice constants, as discussed in the caption of Table I.

	PBE+U	PBE	PBEsol+U	PBEsol	HSE	SCAN
MRE	1.64%	0.64%	0.25%	−0.73%	−0.37%	−0.51%
MARE	1.64%	0.66%	0.53%	0.79%	0.62%	0.68%

configurations given in Fig. 1, and overall favor alternate AFM configurations with clusters of nearest-neighbor aligned spins, contrary to what could be expected on the basis of oxygen-mediated superexchange governing the antiferromagnetism in MnO_2. In contrast to the +U functionals, PBE, PBEsol, and SCAN favor the AFM configuration in β, R, α, and γ, and give essentially degenerate results for the AFM and FM configurations in δ and λ, likely due to the fact that the size of the true antiferromagnetic ground state unit cell in these phases includes up to 128 spins [67,43] the enumeration of which is beyond the scope of this work.

A final measure of functional accuracy is its ability to reproduce lattice parameters, as they are often indicative of how well the functional captures the bonding character of the solid [68,69]. The improved performance of SCAN with respect to lattice constants in comparison to PBE and PBEsol, as can be seen in Table II, follows from the fact that SCAN yields a superior description of both the bonds within the MnO_6 octahedral environment and the weak electron density overlap between octahedra. It is worth noting the exceptional performance of PBEsol+U in reproducing the lattice constants here. While PBEsol underestimates lattice constants, the +U modification typically leads to larger lattice parameters by reducing the electronic overlap between atoms, counteracting the error in PBEsol. Consequently, PBEsol+U is able to minimize the lattice constant error for an optimal choice of U value [19].

For all the properties of MnO_2 that we have considered (polymorph formation energy, band gap, magnetization, and lattice constants), we find that SCAN is the only functional to give high-quality, *ab initio* results in agreement with experiment across the board. In contrast, the empirically fitted PBEsol+U functional performs as well as or better than SCAN on band gaps and lattice constants, but mispredicts the polymorph order and the magnetic character of the system. PBEsol performs well on the polymorph order and magnetization, but significantly underestimates lattice constants and band gaps. HSE, while being much more computationally expensive than all other functionals tested here, only performs well on lattice constants. The consistent agreement between SCAN and experimental results across multiple properties suggests that SCAN, more so than other functionals, is able to capture the physics governing the system rather than acting as a fortuitous correction that improves a target property. We propose that the reason for this superior and consistent performance lies in the design features of SCAN—its built-in agreement with numerous limiting constraints on the exchange-correlation energy, and the inclusion of appropriate norms for which semilocal functionals can be exact or nearly exact, which serve to guide the functional from one constraint to another. We expect similarly positive results on other transition metal oxides with high spin configurations and less than half-full d shells, and somewhat worse results in more self-interaction–dominated systems. However, much more extensive calculations are needed to fully explore the accuracy of SCAN across other chemical spaces.

In conclusion, we have investigated the accuracy of several common DFT functionals, as well as the recently introduced SCAN meta-GGA, with respect to their ability to reproduce key properties of the challenging MnO_2 system. Specifically, we looked at the relative stability, band gaps, magnetic structure, and lattice constants of the β, R, α, γ, λ, and δ phases of MnO_2. We found that although each individual property can be reproduced to good agreement with experiment by several functionals, only SCAN gives quantitatively reliable results for all properties at once. The accuracy, reliability, and computational efficiency of this new functional opens the door to the rigorous theoretical study of the manganese oxide system, from its still-uncertain basic physics to the complex mechanisms underlying the rich catalytic, electrochemical, and optoelectronic behavior of this material.

The work of D.A.K., Y.L., and G.C. is supported by the Center for Next-Generation of Materials by Design, an Energy Frontier Research Center funded by U.S. Department of Energy, Office of Basic Energy Science. The work of H.P., J.S., and J.P.P. is supported as part of the Center for the Computational Design of Functional Layered Materials, an Energy Frontier Research Center funded by the U.S. Department of Energy, Office of Basic Energy Science, under Award No. DE-SC0012575.

[1] W. Kohn and L. J. Sham, Phys. Rev. **140**, A1133 (1965).
[2] A. R. Oganov and C. W. Glass, J. Chem. Phys. **124** 244704 (2006).
[3] S. M. Woodley and R. Catlow, Nat. Mater. **7**, 937 (2008).
[4] D. Spagnoli, K. Refson, K. Wright, and J. D. Gale, Phys. Rev. B **81**, 094106 (2010).
[5] M. T. Curnan and J. R. Kitchin, J. Phys. Chem. C **119**, 21060 (2015).
[6] S. Curtarolo, D. Morgan, and G. Ceder, Calphad **29**, 163 (2005).
[7] J. E. Post, Proc. Natl. Acad. Sci. USA **96**, 3447 (1999).
[8] S. Fritsch, J. E. Post, and A. Navrotsky, Geochim. Cosmochim. Acta **61**, 2613 (1997).

[9] S. Fritsch, J. E. Post, S. L. Suib, and A. Navrotsky, Chem. Mater. **10**, 474 (1998).
[10] L. Hill and A. Verbaere, J. Solid State Chem. **177**, 4706 (2004).
[11] J. C. Hunter, J. Solid State Chem. **39**, 142 (1981).
[12] Y. Kondrashev and A. Zaslavskii, Izv. Akad. Nauk USSR **15**, 179 (1951).
[13] W. Wei, X. Cui, W. Chen, and D. G. Ivey, Chem. Soc. Rev. **40**, 1697 (2011).
[14] D. M. Robinson, Y. B. Go, M. Mui, G. Gardner, Z. Zhang, D. Mastrogiovanni, E. Garfunkel, J. Li, M. Greenblatt, and G. C. Dismukes, J. Am. Chem. Soc. **135**, 3494 (2013).
[15] B. Ammundsen and J. Paulsen, Adv. Mater. **13**, 943 (2001).
[16] C. Franchini, R. Podloucky, J. Paier, M. Marsman, and G. Kresse, Phys. Rev. B **75**, 195128 (2007).
[17] D. Balachandran, D. Morgan, G. Ceder, and A. van de Walle, J. Solid State Chem. **173**, 462 (2003).
[18] T. X. T. Sayle, C. R. A. Catlow, R. R. Maphanga, P. E. Ngoepe, and D. C. Sayle, J. Am. Chem. Soc. **127**, 12828 (2005).
[19] E. Cockayne and L. Li, Chem. Phys. Lett. **544**, 53 (2012).
[20] J. Sun, A. Ruzsinszky, and J. P. Perdew, Phys. Rev. Lett. **115**, 036402 (2015).
[21] J. P. Perdew, K. Burke, and M. Ernzerhof, Phys. Rev. Lett. **77**, 3865 (1996).
[22] J. P. Perdew, A. Ruzsinszky, G. I. Csonka, O. A. Vydrov, G. E. Scuseria, L. A. Constantin, X. Zhou, and K. Burke, Phys. Rev. Lett. **100**, 136406 (2008).
[23] V. I. Anisimov, F. Aryasetiawan, and A. Lichtenstein, J. Phys.: Condens. Matter **9**, 767 (1997).
[24] S. L. Dudarev, G. A. Botton, S. Y. Savrasov, C. J. Humphreys, and A. P. Sutton, Phys. Rev. B **57**, 1505 (1998).
[25] J. Heyd, G. E. Scuseria, and M. Ernzerhof, J. Chem. Phys. **118**, 8207 (2003).
[26] J. Heyd, G. E. Scuseria, and M. Ernzerhof, J. Chem. Phys. **124**, 219906 (2006).
[27] R. Van Noorden, B. Maher, R. Nuzzo *et al.*, Nature (London) **514**, 550 (2014).
[28] V. L. Chevrier, S. P. Ong, R. Armiento, M. K. Y. Chan, and G. Ceder, Phys. Rev. B **82**, 075122 (2010).
[29] G. Hautier, S. P. Ong, A. Jain, C. J. Moore, and G. Ceder, Phys. Rev. B **85**, 155208 (2012).
[30] M. Cococcioni, Rev. Mineral. Geochem. **71**, 147 (2010).
[31] J. P. Perdew, A. Ruzsinszky, G. I. Csonka, O. A. Vydrov, G. E. Scuseria, L. A. Constantin, X. Zhou, and K. Burke, Phys. Rev. Lett. **101**, 239702 (2008).
[32] J. Tao, J. P. Perdew, V. N. Staroverov, and G. E. Scuseria, Phys. Rev. Lett. **91**, 146401 (2003).
[33] Y. Zhao and D. G. Truhlar, J. Chem. Phys. **125**, 194101 (2006).
[34] J. Sun, B. Xiao, and A. Ruzsinszky, J. Chem. Phys. **137**, 051101 (2012).
[35] J. M. del Campo, J. L. Gzquez, S. Trickey, and A. Vela, Chem. Phys. Lett. **543**, 179 (2012).
[36] J. Sun, J. P. Perdew, and A. Ruzsinszky, Proc. Natl. Acad. Sci. USA **112**, 685 (2015).
[37] J. Sun, B. Xiao, Y. Fang, R. Haunschild, P. Hao, A. Ruzsinszky, G. I. Csonka, G. E. Scuseria, and J. P. Perdew, Phys. Rev. Lett. **111**, 106401 (2013).
[38] G. Kresse and J. Furthmller, Comput. Mater. Sci. **6**, 15 (1996).
[39] L. Wang, T. Maxisch, and G. Ceder, Phys. Rev. B **73**, 195107 (2006).
[40] Y. Crespo and N. Seriani, Phys. Rev. B **88**, 144428 (2013).
[41] D. A. Tompsett, D. S. Middlemiss, and M. S. Islam, Phys. Rev. B **86**, 205126 (2012).
[42] N. Yamamoto, T. Endo, M. Shimada, and T. Takada, Jpn. J. Appl. Phys. **13**, 723 (1974).
[43] J. E. Greedan, N. P. Raju, A. S. Wills, C. Morin,, S. M. Shaw, and J. N. Reimers, Chem. Mater. **10**, 3058 (1998).
[44] L. Guo, D. Peng, H. Makino, T. Hanada, S. Hong, K. Sumiyama, T. Yao, and K. Inaba, J. Appl. Phys. **90**, 351 (2001).
[45] H. T. Zhu, J. Luo, H. X. Yang, J. K. Liang, G. H. Rao, J. B. Li, and Z. M. Du, J. Phys. Chem. C **112**, 17089 (2008).
[46] W. Setyawan and S. Curtarolo, Comput. Mater. Sci. **49**, 299 (2010).
[47] S. Curtarolo, W. Setyawan, G. L. Hart, M. Jahnatek, R. V. Chepulskii, R. H. Taylor, S. Wang, J. Xue, K. Yang, O. Levy *et al.*, Comput. Mater. Sci. **58**, 218 (2012).
[48] B. A. Pinaud, Z. Chen, D. N. Abram, and T. F. Jaramillo, J. Phys. Chem. C **115**, 11830 (2011).
[49] N. Ohama and Y. Hamaguchi, J. Phys. Soc. Jpn. **30**, 1311 (1971).
[50] W. H. Baur, Acta Crystallogr. Sect. B **32**, 2200 (1976).
[51] A. Bolzan, C. Fong, B. Kennedy, and C. Howard, Austral. J. Chem. **46**, 939 (1993).
[52] G. Bergerhoff, R. Hundt, R. Sievers, and I. Brown, J. Chem. Inform. Comput. Sci. **23**, 66 (1983).
[53] H. Sato, T. Enoki, M. Isobe, and Y. Ueda, Phys. Rev. B **61**, 3563 (2000).
[54] A. F. ul Islam, R. Islam, and K. Khan, J. Mater. Sci.: Mater. Electron. **16**, 203 (2005).
[55] R. Druilhe and J. Suchet, Czech. J. Phys. **17**, 337 (1967).
[56] A. Bystrom, Acta Chem. Scand. **3**, 163 (1949).
[57] H. Miura, H. Kudou, J. H. Choi, and Y. Hariya, J. Faculty Sci., Hokkaido Univ. Ser. 4 **22**, 611 (1990).
[58] J. Post and P. Heaney, Am. Mineral. **89**, 969 (2004).
[59] M. Rossouw, D. Liles, M. Thackeray, W. David, and S. Hull, Mater. Res. Bull. **27**, 221 (1992).
[60] R. Ma, Y. Bando, L. Zhang, and T. Sasaki, Adv. Mater. **16**, 918 (2004).
[61] R. Chen, P. Zavalij, and M. S. Whittingham, Chem. Mater. **8**, 1275 (1996).
[62] J. Sun, R. C. Remsing, Y. Zhang, Z. Sun, A. Ruzsinszky, H. Peng, Z. Yang, A. Paul, U. Waghmare, X. Wu *et al.*, arXiv:1511.01089.
[63] J. P. Perdew and A. Zunger, Phys. Rev. B **23**, 5048 (1981).
[64] A. Yoshimori, J. Phys. Soc. Jpn. **14**, 807 (1959).
[65] H. Sato, K. Wakiya, T. Enoki, T. Kiyama, Y. Wakabayashi, H. Nakao, and Y. Murakami, J. Phys. Soc. Jpn. **70**, 37 (2001).
[66] M. Regulski, R. Przeniosło, I. Sosnowska, and J.-U. Hoffmann, Phys. Rev. B **68**, 172401 (2003).
[67] D. Morgan, B. Wang, G. Ceder, and A. van de Walle, Phys. Rev. B **67**, 134404 (2003).
[68] P. Haas, F. Tran, and P. Blaha, Phys. Rev. B **79**, 085104 (2009).
[69] G. I. Csonka, J. P. Perdew, A. Ruzsinszky, P. H. T. Philipsen, S. Lebègue, J. Paier, O. A. Vydrov, and J. G. Ángyán, Phys. Rev. B **79**, 155107 (2009).